GA–A27243

THE ROLE OF ZONAL FLOWS AND PREDATOR-PREY OSCILLATIONS IN THE FORMATION OF CORE AND EDGE TRANSPORT BARRIERS

by
L. SCHMITZ, L. ZENG, T.L. RHODES, J.C. HILLESHEIM,
W.A. PEEBLES, R.J. GROEBNER, K.H. BURRELL,
E.J. DOYLE, W.M. SOLOMON and G. WANG

APRIL 2012

GENERAL ATOMICS

DISCLAIMER

This report was prepared as an account of work sponsored by an agency of the United States Government. Neither the United States Government nor any agency thereof, nor any of their employees, makes any warranty, express or implied, or assumes any legal liability or responsibility for the accuracy, completeness, or usefulness of any information, apparatus, product, or process disclosed, or represents that its use would not infringe privately owned rights. Reference herein to any specific commercial product, process, or service by trade name, trademark, manufacturer, or otherwise, does not necessarily constitute or imply its endorsement, recommendation, or favoring by the United States Government or any agency thereof. The views and opinions of authors expressed herein do not necessarily state or reflect those of the United States Government or any agency thereof.

GA–A27243

THE ROLE OF ZONAL FLOWS AND PREDATOR-PREY OSCILLATIONS IN THE FORMATION OF CORE AND EDGE TRANSPORT BARRIERS

by
L. SCHMITZ,* L. ZENG,* T.L. RHODES,* J.C. HILLESHEIM,*
W.A. PEEBLES,* R.J. GROEBNER, K.H. BURRELL,
E.J. DOYLE,* W.M. SOLOMON† and G. WANG*

This is a preprint of a paper to be presented at the 24th IAEA Fusion Energy Conference, October 8–13, 2012 in San Diego, California and to be published in Proceedings.

*University of California-Los Angeles, Los Angeles, California USA
†Princeton Plasma Physics Lab, Princeton, New Jersey USA

Work supported by the
U.S. Department of Energy under
DE-FG02-08ER54984, DE-FG03-01ER54615,
DE-FC02-04ER54698 and DE-AC02-09CH11466

GENERAL ATOMICS PROJECT 30200
APRIL 2012

GENERAL ATOMICS

Understanding the formation dynamics of core and edge transport barriers is of crucial importance for extrapolating present tokamak performance to burning plasma regimes. We present here direct evidence of low frequency Zonal Flows (ZF) reducing electron-scale turbulence in an electron internal transport barrier (ITB) at the q=2 rational surface, and periodically suppressing ITG-scale turbulence via a predator-prey cycle near the separatrix, triggering edge barrier formation. Multi-channel Doppler Backscattering (DBS) revealed strong similarity of the radial structure of the ZF-induced shear layer, the ratio of the $\mathbf{E}\times\mathbf{B}$ shearing rate $\omega_{\mathbf{ExB}}$ to the turbulence decorrelation rate $\Delta\omega_D$, and the phase shift between turbulence envelope and time-dependent flow shear, in both barrier types.

Electron-scale ($k_\theta\rho_s\sim3$) turbulence suppression by ZF shear has been directly observed for the first time in an electron ITB [Fig. 1(a–c)]. A fine-scale, ZF-induced radial double shear layer with positive outboard and negative inboard $\mathbf{E}\times\mathbf{B}$ flow shear [$\Delta r\sim4\rho_s\sim1.5$–2 cm, Fig. 2(b)] is observed at the q=2 surface. In contrast to earlier observations of turbulence suppression in ion ITBs near q=2 [1], no barrier is present here in the ion temperature (or density) profile; hence the shear layer is not related to a local increase in the ion pressure gradient. The ZF is composed of steady-state and broadband components (with a frequency spectrum $f_{ZF}\leq5$ kHz). Anti-correlation of ZF shear and density fluctuation amplitude is found [Fig. 2(d)]. In both the electron ITB and the edge barrier discussed below, turbulence reduction/quenching is observed in the inner and outer shear flow layers, with an embedded shear-free zone where the turbulence decorrelation rate remains above the flow shearing rate.

Near the L-H transition power threshold (~4 MW neutral beam co-injection with L-mode plasma density $\langle n\rangle\sim2.5\times10^{13}$ cm^{-3}), ZFs are observed to trigger edge barrier formation via extended limit cycle oscillations (LCO) between the density fluctuation envelope ñ, (with $k_\theta\rho_s\sim0.5\pm0.2$) and the $\mathbf{E}\times\mathbf{B}$ velocity at/inside the last closed flux surface (LCFS) [Fig. 2(a,b)] [2]. The ZF flow shear periodically suppresses turbulence. The turbulence level then increases once the ZF is damped. The D_α recycling light indicates enhanced particle outflux following the peak in density fluctuation amplitude [Fig. 2(c)]. $\mathbf{E}\times\mathbf{B}$ flow oscillations lag ñ by 90º as seen in Fig. 1(d) (magenta/purple data points taken during a 3 ms time interval starting at t=1278 ms, 1 and 2.5 cm inside the LCFS; green points correspond to L-mode, red points to H-mode). Equilibrium $\mathbf{E}\times\mathbf{B}$ shear due to the increasing edge ion pressure gradient becomes important after t=1280 ms during the LCO [Fig. 1(a)], changing the phase shift between ñ and $\omega_{\mathbf{ExB}}$ gradually from 90º to 180º, and lengthening the limit cycle period. Both features are consistent with a two predator, one prey model of the L-H transition with equilibrium shear locking in the final transition [3], as will be shown in a comparison of experimental results with a 0-D Lotka-Volterra model

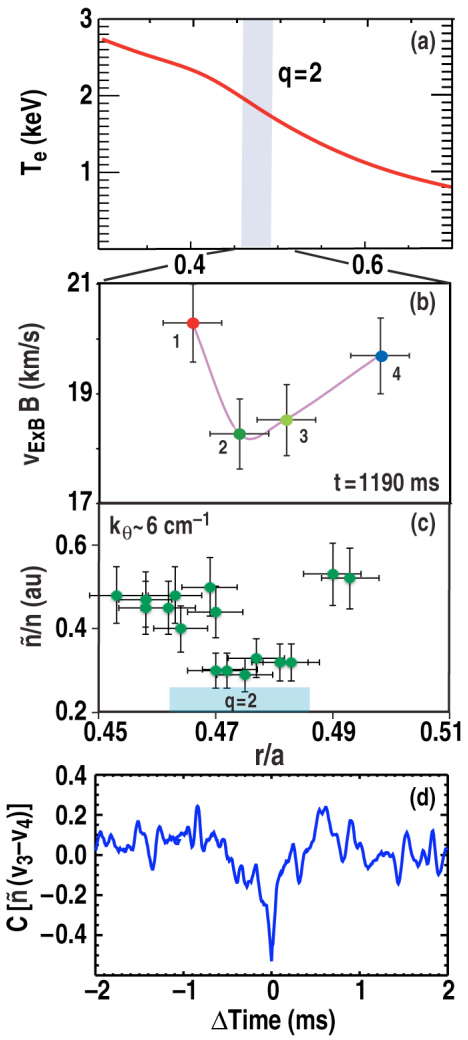

Fig. 1. (a) Radial electron temperature profile showing internal transport barrier; (b) radial profile of v_{ExB}; (c) radial profile of rms density fluctuation level ñ; (d) correlation coefficient of ω_{ExB} and ñ at r/a ~0.5.

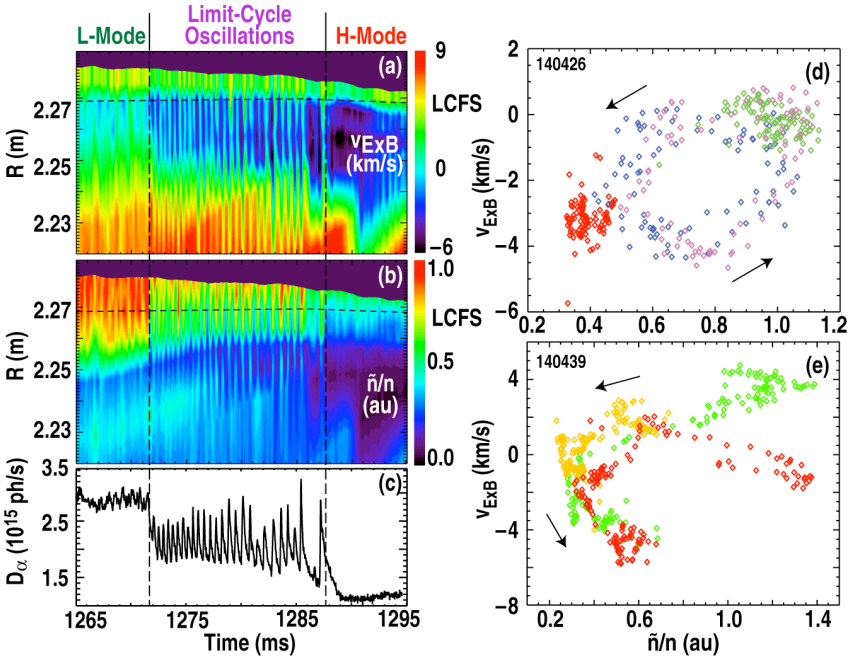

Fig. 2. Time evolution of (a) **ExB** velocity; (b) relative density fluctuation level ñ/n; (c) divertor D_α signal; (d) ñ - v_{ExB} limit cycle corresponding to (a,b); (e) limit cycle in a regular L-H transition.

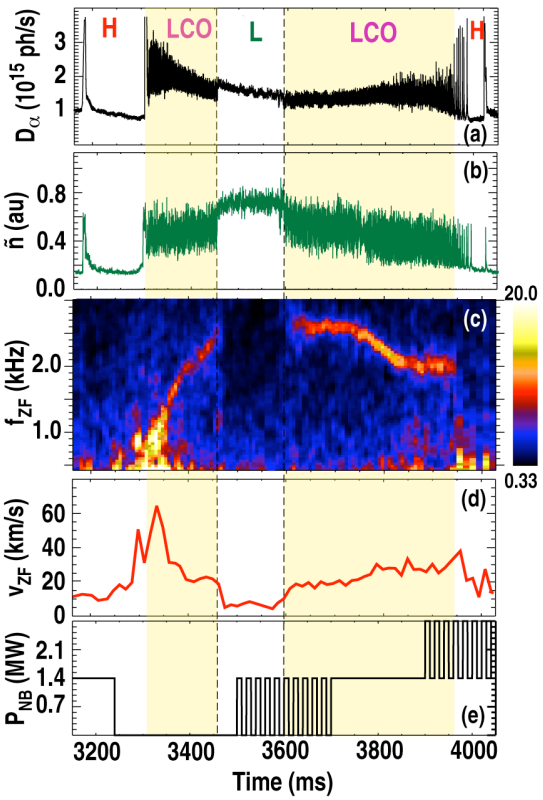

Fig. 3. (a) D_α recycling light, (b) ñ; (c) ZF (LCO) frequency spectrum; (d) magnitude of ZF **E × B** velocity, and (e) neutral beam power during H-L and L-H transitions with LCO.

including pressure profile evolution. In a regular L-H transition in the same lower single null divertor configuration (140439), but with beam power above threshold (L-mode density ‹n›~1.5x 10^{13} cm^{-3}), ZFs are documented here for the first time as short transients executing only part of one limit cycle period over ~1.5 ms [Fig. 1(e), showing three data sets for major radii 0.5–4 cm inside the LCFS]. Turbulence suppression due to ZF shearing is first observed in both transition types near the separatrix when the turbulence decorrelation rate $\Delta\omega_D$ decreases sharply concomitantly with an increasing **E × B** shearing rate ω_{ExB} due to ZF onset.

Limit cycle H-L back-transitions, recently observed in DIII-D [Fig. 3(a,b)] after beam power shutoff [Fig. 3(e)], are potentially important for ITER as a tool for controlled, gradual reduction of β_θ during current ramp-down. In DIII-D, during the back transition the LCO/ZF frequency increases, and the ZF amplitude decreases [Fig. 3(c,d)], reversing the forward transition sequence, while preserving the 90º phase lag of ω_{ExB} with respect to ñ. In the data shown, a forward L-H transition with LCO follows as beam power is increased again.

This work was supported in part by the U.S. Department of Energy under DE-FG02-08ER54984, DE-FG03-01ER54615, DE-FC02-04ER54698 and DE-AC02-09CH11466.

[1] M. Austin, et al., Phys. Plasmas **13**, 082502 (2006).

[2] L. Schmitz, L. Zeng, et al., "The Role of Zonal Flow Predator-Prey Oscillations in Triggering the Transition to H-Mode Confinement," accepted for publication in Phys. Rev. Lett. 2012.

[3] E.J. Kim and P.H. Diamond, Phys. Rev. Lett. **90**, 185006 (2003).